J|A|C|S
ARTICLES
Published on Web 08/10/2006

Early Intermediate in Human Prion Protein Folding As Evidenced by Ultrarapid Mixing Experiments

Adrian C. Apetri,[‡,#] Kosuke Maki,[†,§] Heinrich Roder,*[,†] and Witold K. Surewicz*[,‡]

Contribution from the Department of Physiology and Biophysics, Case Western Reserve University, Cleveland, Ohio 44106, and Basic Science Division, Fox Chase Cancer Center, Philadelphia, Pennsylvania 19111

Received June 2, 2006; E-mail: roder@fccc.edu; wks3@case.edu

Abstract: An important step toward understanding the mechanism of the PrP^{C}-to-PrP^{Sc} conversion is to elucidate the folding pathway(s) of the prion protein. On the basis of stopped-flow measurements, we recently proposed that the prion protein folds via a transient intermediate formed on the submillisecond time scale, and mutations linked to familial diseases result in a pronounced increase in the population of this intermediate. Here, we have extended these studies to continuous-flow measurements using a capillary mixing system with a time resolution of ~100 μs. This allowed us to directly observe two distinct phases in folding of the recombinant human prion protein 90-231, providing unambiguous evidence for rapid accumulation of an early intermediate (with a time constant of ~50 μs), followed by a rate-limiting folding step (with a time constant of ~700 μs). The present study also clearly demonstrates that the population of the intermediate is significantly increased at mildly acidic pH and in the presence of urea. A similar three-state folding behavior was observed for the Gerstmann−Straussler−Scheinker disease-associated F198S mutant, in which case the population of an intermediate was greatly increased as compared to that of the wild-type protein. Overall, the present data strongly suggest that this partially structured intermediate may be a direct monomeric precursor of the misfolded PrP^{Sc} oligomer.

Introduction

Prion diseases, or transmissible spongiform encephalopathies (TSEs), are fatal neurodegenerative disorders that include scrapie in sheep, bovine spongiform encephalopathy in cattle, chronic wasting disease in cervids, and Creutzfeldt−Jakob disease, Gerstmann−Straussler−Scheinker disease, and fatal familial insomnia in humans.[1−7] All of these diseases, including those that arise spontaneously, by genetic mutation, or by infection, are associated with the conformational conversion of a normal (cellular) prion protein, PrP^{C}, into a misfolded isoform, PrP^{Sc}. According to the "protein-only" hypothesis, PrP^{Sc} itself is the infectious TSE pathogen; it is believed to self-perpetuate by a mechanism involving binding to PrP^{C} and the recruitment of the latter protein to the PrP^{Sc} state.[1,2] Though not universally accepted, this model is supported by a wealth of experimental observations,[1−9] including the recent success in generating infectious PrP^{Sc} in vitro.[10,11] Furthermore, the general concept that proteins alone can act as infectious agents has been proven in recent studies on conformation-based prion inheritance in yeast and fungi.[12−14]

PrP^{C} is a 231-residue glycoprotein composed of a highly flexible N-terminal part and a globular C-terminal domain comprising three α-helices and two very short β-strands.[15−18] Although they appear to have identical covalent structures,[19] PrP^{C} and PrP^{Sc} differ profoundly in their biophysical properties. PrP^{C} is monomeric, proteinase-sensitive, and soluble in nonionic detergents, whereas PrP^{Sc} is oligomeric, partially resistant to proteinase digestion, and highly insoluble.[1−7] Furthermore, in contrast to the largely α-helical PrP^{C}, the pathogenic PrP^{Sc}

‡ Case Western Reserve University.
† Fox Chase Cancer Center.
# Current address: Howard Hughes Medical Institute, Yale University, New Haven, CT.
§ Current address: Department of Physics, University of Tokyo, Tokyo 113-0033, Japan.

(1) Prusiner, S. B. *Science* **1982**, *216* (4542), 136−44.
(2) Prusiner, S. B. *Proc. Natl. Acad. Sci. U.S.A.* **1998**, *95*, 13363−83.
(3) Caughey, B. *Trends Biochem. Sci.* **2001**, *26*, 235−42.
(4) Caughey, B.; Chesebro, B. *Adv. Virus Res.* **2001**, *56*, 277−311.
(5) Collinge, J. *Annu. Rev. Neurosci.* **2001**, *24*, 519−50.
(6) Aguzzi, A.; Polymenidou, M. *Cell* **2004**, *116*, 313−27.
(7) Weissmann, C. *Nat. Rev. Microbiol.* **2004**, *2*, 861−71.
(8) Jones, E. M.; Surewicz, W. K. *Cell* **2005**, *121*, 63−72.
(9) Surewicz, W. K.; Jones, E. M.; Apetri, A. C. *Acc. Chem. Res.*, published online May 19, 2006, http://dx.doi.org/10.1021/ar050226c.
(10) Castilla, J.; Saa, P.; Hetz, C.; Soto, C. *Cell* **2005**, *121*, 195−206.
(11) Legname, G.; Baskakov, I. V.; Nguyen, H. O.; Riesner, D.; Cohen, F. E.; DeArmond, S. J.; Prusiner, S. B. *Science* **2004**, *305*, 673−6.
(12) Tanaka, M.; Chien, P.; Naber, N.; Cooke, R.; Weissman, J. S. *Nature* **2004**, *428*, 323−8.
(13) King, C. Y.; Diaz-Avalos, R. *Nature* **2004**, *428*, 319−23.
(14) Chien, P.; Weissman, J. S.; DePace, A. H. *Annu. Rev. Biochem.* **2004**, *73*, 617−56.
(15) Riek, R.; Hornemann, S.; Wider, G.; Billeter, M.; Glockshuber, R.; Wuthrich, K. *Nature* **1996**, *382*, 180−2.
(16) Zahn, R.; Liu, A.; Luhrs, T.; Riek, R.; von Schroetter, C.; Lopez Garcia, F.; Billeter, M.; Calzolai, L.; Wider, G.; Wuthrich, K. *Proc. Natl. Acad. Sci. U.S.A.* **2000**, *97*, 145−50.
(17) Liu, H.; Farr-Jones, S.; Ulyanov, N. B.; Llinas, M.; Marqusee, S.; Groth, D.; Cohen, F. E.; Prusiner, S. B.; James, T. L. *Biochemistry* **1999**, *38*, 5362−77.
(18) Donne, D. G.; Viles, J. H.; Groth, D.; Mehlhorn, I.; James, T. L.; Cohen, F. E.; Prusiner, S. B.; Wright, P. E.; Dyson, H. J. *Proc. Natl. Acad. Sci. U.S.A.* **1997**, *94*, 13452−7.
(19) Stahl, N.; Baldwin, M. A.; Teplow, D. B.; Hood, L.; Gibson, B. W.; Burlingame, A. L.; Prusiner, S. B. *Biochemistry* **1993**, *32*, 1991−2002.

appears to have a high content of β-sheet structure,[20,21] although no high-resolution structural data is yet available for the latter conformer.

Despite numerous studies, little is known about the mechanism of the $PrP^{C} \rightarrow PrP^{Sc}$ conversion. An important step toward understanding this mechanism is to elucidate the folding pathway(s) of the prion protein in an effort to identify the direct monomeric precursor of the oligomeric PrP^{Sc} species. While initial experiments suggested that the prion protein folds very rapidly by a two-state mechanism,[22] our recent kinetic stopped-flow studies using single-Trp variants of huPrP90-231 revealed that, during refolding from urea, the human prion protein populates a partially structured intermediate.[23,24] This early intermediate, which accumulates within the dead time of stopped-flow experiments (~1 ms), was detected by an incomplete recovery of the fluorescence amplitude upon extrapolation of experimental data to time zero (the presence of a so-called burst phase), as well as a well-defined slope change in a plot of the logarithm of the rate constant for folding versus urea concentration (chevron plot). While the above criteria have been widely used to detect and characterize intermediates in protein folding,[25−27] some authors argue that there might be alternative explanations for the presence of burst phases and nonlinearities in chevron plots.[28,29] Therefore, in an attempt to obtain a more direct evidence for the population of the intermediate ensemble in prion protein folding, we have extended our kinetic studies to measurements using a continuous-flow capillary mixing instrument.[30] This instrumentation makes it possible to measure the kinetics of folding on a substantially shorter time scale as compared to conventional stopped-flow methods.[31] The present data provide unambiguous evidence for an early intermediate which accumulates on the time scale of hundreds of microseconds, followed by a rate-limiting folding step on the millisecond time scale**.** Furthermore, continuous-flow experiments demonstrate a greatly increased population of the intermediate for the disease-related prion protein mutant, reinforcing our hypothesis that the intermediate state may represent a crucial monomeric precursor of PrP^{Sc} aggregates.

Materials and Methods

Protein Expression and Purification. The plasmid encoding huPrP90-231 with an N-terminal linker containing a His-6 tail and a thrombin cleavage site was described previously.[32,33] The W99F/Y218W huPrP90-231 variant was constructed by site-directed mutagenesis using appropriate primers and the QuikChange kit (Stratgene). The proteins were expressed, cleaved with thrombin, and purified according to the previously described protocol.[32,34] The concentration of purified protein was determined spectrophotometrically using the molar extinction coefficient, ϵ_{276}, of 21 640 M^{-1} cm^{-1}.

Continuous-Flow Measurements. The proteins were first fully unfolded in 6 M urea buffered with 20 mM Gly-HCl, pH 3. The kinetics of the refolding reactions were studied by diluting the fully unfolded protein at a 1:10 ratio into refolding buffer (50 mM phosphate, pH 7.0, or 50 mM sodium acetate, pH 4.8) containing urea at a desired concentration. In most experiments, the final protein concentration was 40 μM. The reactions were monitored at 5 °C by fluorescence above 324 nm (excitation at 288 nm) using the continuous-flow capillary mixing method described by Shastry et al.[30] at total flow rates of 0.825 and 1.375 mL/s. The dead time of the capillary mixer was determined by measuring the quenching of *N*-acetyl tryptophan amide fluorescence by *N*-bromosuccinimide at several quencher concentrations. Under our present experimental conditions (5 °C; final urea concentration of ~0.6 M), the measured dead times at 0.825 and 1.375 mL/s total flow rates were 180 and 120 μs, respectively. Each protein refolding reaction was measured at least five times. The kinetic data were numerically analyzed according to a three-state sequential model (Scheme 1, below) using a rate-matrix algorithm implemented in IGOR Pro software (Wavemetrics Inc). We also made the conventional assumption that there is a linear dependence between the logarithm of an elementary rate constant, k_{ij}, and denaturant concentration:

$$\log k_{ij} = \log k_{ij}^{0} + (m_{ij}/RT)[\text{urea}] \quad (1)$$

where k_{ij}^{0} and m_{ij} represent the microscopic rate constant in the absence of denaturant and the urea dependence of the rate constant, respectively.

The observed rate constants and corresponding amplitudes were obtained directly from the best fit of the kinetic traces at each denaturant concentration. The elementary rate constants and *m* values were systematically varied to obtain a satisfactory match between calculated and measured data, as previously described.[35]

According to the three-state model (Scheme 1, below), the temporal evolution of native (N), intermediate (I), and unfolded (U) species under a particular set of experimental conditions can be described in terms of a system of three differential equations.[36] The solutions are sums of two exponential terms describing the dependence of the populations of N, I, and U on reaction time and denaturant concentration. The time-dependent accumulation of N, I, and U was modeled at 0, 1, 2, and 4 M urea using an IGOR Pro routine as previously described.[36]

Results

Double-Exponential Folding of huPrP90-231. As in our previous stopped-flow experiments,[23,24] the present studies were performed using huPrP90-231 variant with a single Trp residue introduced by a conservative replacement of Tyr at position 218. The protein was first denatured in 6 M urea at pH 3, and refolding was triggered by rapid 1:10 dilution to 50 mM phosphate buffer, pH 7, containing various concentrations of the denaturant (0.7−3.5 M urea). The progress of the reaction was followed at 5 °C using the continuous-flow method by monitoring the decay of fluorescence of Trp 218, which is highly quenched in the native state.[23] Since the refolding reactions were not completed within the time frame of the continuous-flow experiment (i.e., ~500 μs), the flow-through from kinetic measurements was collected, and its fluorescence was measured at a later time by passing it through the capillary system. The final fluorescence amplitudes obtained in this manner were used

(20) Caughey, B. W.; Dong, A.; Bhat, K. S.; Ernst, D.; Hayes, S. F.; Caughey, W. S. *Biochemistry* **1991**, *30*, 7672−80.
(21) Pan, K.; Baldwin, M.; Nguyen, J.; Gasset, M.; Serban, A.; Groth, D.; Mehlhorn, I.; Huang, Z.; Fletterick, R. J.; Cohen, F. E.; Prusiner, S. B. *Proc. Natl. Acad. Sci. U.S.A.* **1993**, *90*, 10962−6.
(22) Wildegger, G.; Liemann, S.; Glockshuber, R. *Nat. Struct. Biol.* **1999**, *6*, 550−3.
(23) Apetri, A. C.; Surewicz, W. K. *J. Biol. Chem.* **2002**, *277*, 44589−92.
(24) Apetri, A. C.; Surewicz, K.; Surewicz, W. K. *J. Biol. Chem.* **2004**, *279*, 18008−14.
(25) Park, S. H.; O'Neil, K. T.; Roder, H. *Biochemistry* **1997**, *36*, 14277−83.
(26) Ferguson, N.; Capaldi, A. P.; James, R.; Kleanthous, C.; Radford, S. E. *J. Mol. Biol.* **1999**, *286*, 1597−608.
(27) Sanchez, I. E.; Kiefhaber, T. *J. Mol. Biol.* **2003**, *325*, 367−76.
(28) Oliveberg, M. *Acc. Chem. Res.* **1998**, *31*, 765−72.
(29) Krantz, B. A.; Mayne, L.; Rumbley, J.; Englander, S. W.; Sosnick, T. R. *J. Mol. Biol.* **2002**, *324*, 359−71.
(30) Shastry, M. C.; Luck, S. D.; Roder, H. *Biophys. J.* **1998**, *74*, 2714−21.
(31) Roder, H.; Maki, K.; Cheng, H. *Chem. Rev.* **2006**, *106*, 1836−61.
(32) Morillas, M.; Swietnicki, W.; Gambetti, P.; Surewicz, W. K. *J. Biol. Chem.* **1999**, *274*, 36859−65.
(33) Morillas, M.; Vanik, D. L.; Surewicz, W. K. *Biochemistry* **2001**, *40*, 6982−7.
(34) Zahn, R.; von Schroetter, C.; Wuthrich, K. *FEBS Lett.* **1997**, *417*, 400−4.
(35) Khorasanizadeh, S.; Peters, I. D.; Roder, H. *Nat. Struct. Biol.* **1996**, *3*, 193−205.
(36) Teilum, K.; Maki, K.; Kragelund, B. B.; Poulsen, F. M.; Roder, H. *Proc. Natl. Acad. Sci. U.S.A.* **2002**, *99*, 9807−12.

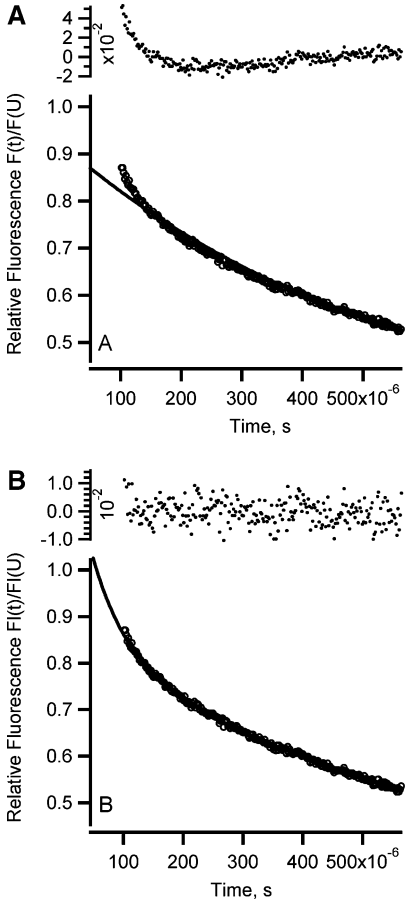

Figure 1. Time course of tryptophan fluorescence changes during the refolding of huPrP90-231 in 50 mM phosphate buffer, pH 7.0, in the presence of 1.1 M urea. The refolding kinetics was measured by continuous-flow mixing at 5 °C and a protein concentration of 40 μM. Solid lines represent the best fit of the kinetic data to a single-exponential (A) and double-exponential function (B). The residuals of the fits are shown above kinetic traces. The equilibrium fluorescence value for the native state was used as a constraint for both the single- and double-exponential fits.

as constraints for fitting the exponential decays corresponding to the refolding of huPrP90-231.

Figure 1 shows a representative kinetic trace for the refolding of huPrP90-231 in the presence of 1.1 M urea, together with best fits to single- and double-exponential functions and residuals of these fits. While the fit to a single exponential is very poor (Figure 1A), the kinetic trace is well described by a sum of two exponential phases with time constants of 19 000 and 1400 s^{-1} (Figure 1B). A similar situation was encountered for refolding curves at other urea concentrations studied; in each case, the continuous-flow kinetic traces could not be fit to a single-exponential function, whereas the double-exponential fits were very good (Figure 2). Such a double-exponential character of kinetics traces clearly indicates the accumulation of an intermediate during prion protein folding, with the fast phase corresponding to the formation of an intermediate ensemble and the slower phases corresponding to the rate-limiting step of native state formation.

Figure 3 shows the rate constants corresponding to the two folding phases resolved in continuous-flow experiments, plotted (on a semilogarithmic scale) as a function of denaturant concentration, together with the rate constants obtained in our previous stopped-flow measurements.[23] Importantly, the rate constants for the slower phase in continuous-flow traces are

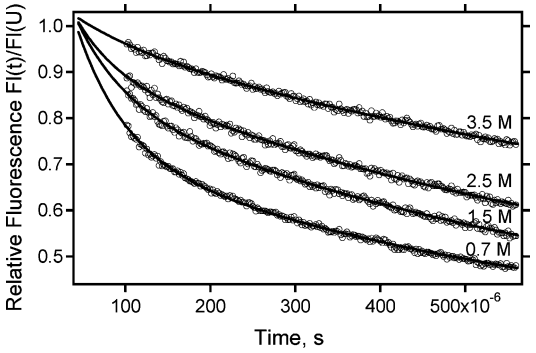

Figure 2. Representative continuous-flow kinetic traces for huPrP90-231 refolding in varying concentrations of urea at pH 7 (50 mM phosphate buffer). Solid lines represent the best fit of kinetic traces to a double-exponential function. Numbers at each curve indicate final concentrations of urea.

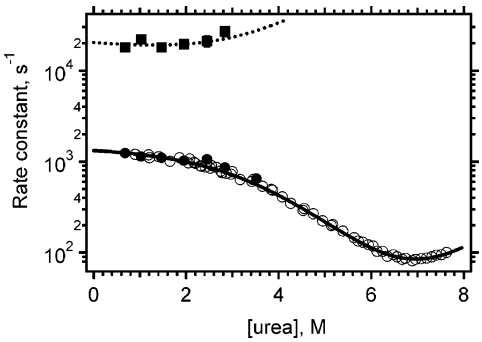

Figure 3. Urea concentration dependence of rate constants for folding/unfolding of huPrP90-231 at pH 7. (■) and (●) represent rate constants for fast and slow refolding phases, respectively, as observed in continuous-flow experiments; (○) represent rate constants for the single folding/unfolding phase observed in stopped-flow experiments. All rate constants were measured at 5 °C in 50 mM phosphate buffer, pH 7. Lines represent the best fit according to a three-state folding model (Scheme 1).

essentially identical to the rates measured in stopped-flow experiments. This close match provides an internal control for the validity of our kinetic data. The observed rate constants for the fast and slow phases (λ_1 and λ_2) could be well modeled according to a three-state scheme

Scheme 1

$$\mathrm{U} \underset{k_{\mathrm{IU}}}{\overset{k_{\mathrm{UI}}}{\rightleftharpoons}} \mathrm{I} \underset{k_{\mathrm{NI}}}{\overset{k_{\mathrm{IN}}}{\rightleftharpoons}} \mathrm{N}$$

where U and N represent the unfolded and native states, respectively, and I represents an on-path folding intermediate. The fit in Figure 3 was obtained by systematic variation of the elementary rate constants (k_{ij}) in the absence of denaturant and their dependence on urea concentration (m_{ij}) (see eq 1, above). The kinetic parameters derived from the best fit of the present data, together with those obtained from previous stopped-flow experiments, are listed in Table 1. Since the fast phase was not directly observed in the stopped-flow experiments, we previously could determine only the pre-equilibrium constant (K_{UI}) and the corresponding m value (m_{UI}) for the U ↔ I transition.[23] With a complete set of kinetic data provided by continuous-flow measurements, it is now possible to determine the individual elementary rate constants, k_{UI} and k_{IU}, and the corresponding $m_{\mathrm{UI}}^{\ddagger}$ and $m_{\mathrm{IU}}^{\ddagger}$ values (Table 1). Importantly, the equilibrium m value, $m_{\mathrm{UI}} = m_{\mathrm{UI}}^{\ddagger} + m_{\mathrm{IU}}^{\ddagger} = 2.1$ kJ mol^{-1} M^{-1}, is identical to the m_{UI} parameter obtained previously from our

Table 1. Thermodynamic and Kinetic Parameters for the Folding of huPrP90-231[a]

	WT			F198S		
	CF + SF	SF	equilibrium	CF + SF	SF	equilibrium
k_{UI}^0	19500			18000		
$m_{UI}^{\ddagger}$	0.3			1.5		
k_{IU}^0	880			409		
$m_{IU}^{\ddagger}$	1.8			0.9		
k_{IN}^0	1390	1290		1500	1150	
$m_{IN}^{\ddagger}$	0.2	0.2		0.3	0.12	
k_{NI}^0	0.2	0.03		6.5	3.3	
$m_{NI}^{\ddagger}$	1.8	2.4		1.2	1.4	
ΔG_{UI}	7.1	5.8		8.6	7.0	
m_{UI}	2.1	2.1		2.4	2.5	
ΔG_{UN}	28.0	30.7	29.4 ± 1.2	21.3	20.5	21.6 ± 1.1
m_{eq}	4.1	4.4	4.3	3.9	4.0	4.0

[a] Rates are given in s^{-1}, m values in kJ mol^{-1} M^{-1}, and ΔG values in kJ mol^{-1}. The rate constants and their associated m values were determined from the fits shown in Figures 3 and 4, based on the model depicted in Scheme 1. For continuous-flow experiments, the equilibrium m value was calculated as the sum of individual m_{ij} values corresponding to the four elementary rate constants ($m_{eq} = m_{UI}^{\ddagger} + m_{IU}^{\ddagger} + m_{IN}^{\ddagger} + m_{NI}^{\ddagger}$) and the global free energy according to the formula $\Delta G_{UN} = \Delta G_{UI} + \Delta G_{IN}$, where $\Delta G_{UI} = RT \ln(k_{UI}/k_{IU})$ and $\Delta G_{IN} = RT \ln(k_{IN}/k_{NI})$. Parameters corresponding to stopped-flow and equilibrium measurements were derived as previously described.[23,24]

pre-equilibrium analysis,[23] and the free energy associated with the U-to-I transition, $\Delta G_{UI} = -RT \ln K_{UI}$, as calculated from the present data, is in reasonably good agreement with our previous estimate based on stopped-flow measurements alone. Moreover, the global m_{eq} and ΔG_{UN} values derived from the kinetic data are very similar to the corresponding parameters obtained from equilibrium experiments, further indicating that the three-state model involving an intermediate ensemble adequately describes the folding of the human prion protein.

Folding of the Disease-Associated F198S Mutant of huPrP90-231. On the basis of our recent stopped-flow data, we have concluded that, for the majority of PrP variants with mutations linked to familial prion diseases, the population of the folding intermediate is much higher as compared to that of the wild-type protein.[24] This led us to the working hypothesis that partially structured momomeric intermediates likely play a crucial role in the $PrP^C \rightarrow PrP^{Sc}$ conversion. To gain further insight into the effect of pathogenic mutations on the prion protein folding pathway, we have extended these studies to continuous-flow measurements. Since these measurements require very large quantities (several hundred milligrams) of highly purified protein, we have focused on one pathogenic variant, F198S, for which the population of the intermediate appears to be especially high.[24] This variant, associated with Gerstmann−Straussler−Scheinker disease, was recently shown to undergo a spontaneous conversion to the scrapie-like form in vitro.[37]

Similar to the wild-type prion protein, the kinetic traces for the refolding of F198S huPrP90-231 could not be approximated as a single exponential but were well represented by a double-exponential function (data not shown for brevity). Furthermore, akin to the wild-type protein, the denaturant dependence of rate constants for this variant could be quantitatively modeled as a three-state folding process according to Scheme 1 (Figure 4), with the elementary rate constants, k_{ij}, and the m_{ij} values listed in Table 1. The ΔG_{UN} and m_{eq} values derived from this three-state fit of the kinetic data are in excellent agreement with those estimated from equilibrium measurements ($\Delta G_{UN} = 21.3$ and 21.6 kJ mol^{-1} and $m_{eq} = 3.9$ and 4.0 kJ mol^{-1} M^{-1}, respectively; see Table 1).

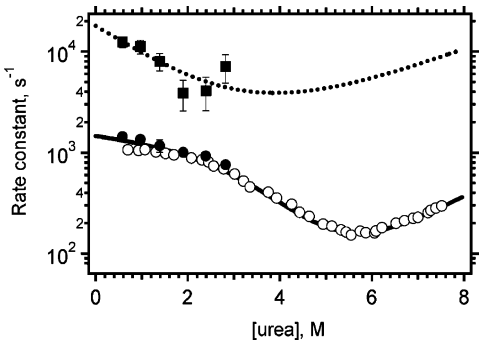

Figure 4. Urea concentration dependence of rate constants for folding/unfolding of the diseases-associated F198S mutant of huPrP90-231 at pH 7. (■) and (●) represent rate constants for fast and slow refolding phases, respectively, as observed in continuous-flow experiments; (○) represent rate constant for the single folding/unfolding phase observed in stopped-flow experiments. All rate constants were measured at 5 °C in 50 mM phosphate buffer, pH 7. Lines represent the best fit according to a three-state folding model (Scheme 1).

The complete set of rate parameters provided by a combination of continuous-flow and stopped-flow experiments allowed us to calculate the time-dependent evolution of each individual state populated during prion protein folding at different denaturant concentrations. The results of such simulations for the population of the intermediate ensemble for wild-type huPrP90-231 and the F198S variant at 0, 1, 2, and 4 M urea are shown in Figure 5. While the time courses of transient changes in the population of the I state for both proteins are similar, the simulations reveal substantial differences in the population of the intermediate when calculations are extended beyond approximately 10 ms. Since the folding reaction of the prion protein is extremely fast (completed within milliseconds), data calculated for longer times (represented as horizontal lines) provide a reliable measure of the population of the I state under equilibrium conditions. Importantly, at each denaturant concentration, the population of the intermediate species for F198S variant is more than 10-fold higher as compared with that of the wild-type protein. For the mutant protein, this population under native buffer conditions is about 1 per 250 molecules; it increases further in the presence of the denaturant, reaching the level of 1:70 and 1:25 molecules in 2 and 4 M urea, respectively. The corresponding values for the wild-type protein are 1:10 000, 1:1100, and 1:300 in the presence of 0, 2, and 4 M urea, respectively. The population of the I state for wild-type huPrP90-231 under native buffer conditions, derived from the present data, is higher than the ~1:40 000 previously estimated on the basis of stopped-flow measurements alone.[24] The present estimate, based on a more complete set of data, is more reliable. It should be noted that, in terms of free energy, this discrepancy is relatively small, corresponding to $\Delta\Delta G_{IN} = 2.7$ kJ mol^{-1}.

Folding Kinetics of huPrP90-231 at Acidic pH. Our previous stopped-flow measurements indicated that the folding intermediate of huPrP90-231 is considerably more stable under mildly acidic conditions (pH 4.8) than at neutral pH.[23] However, since in the stopped-flow experiments at low urea concentrations we were able to recover only a small fraction of kinetic amplitudes, calculations based on these measurements could be

(37) Vanik, D. L.; Surewicz, W. K. *J. Biol. Chem.* **2002**, *277*, 49065−70.

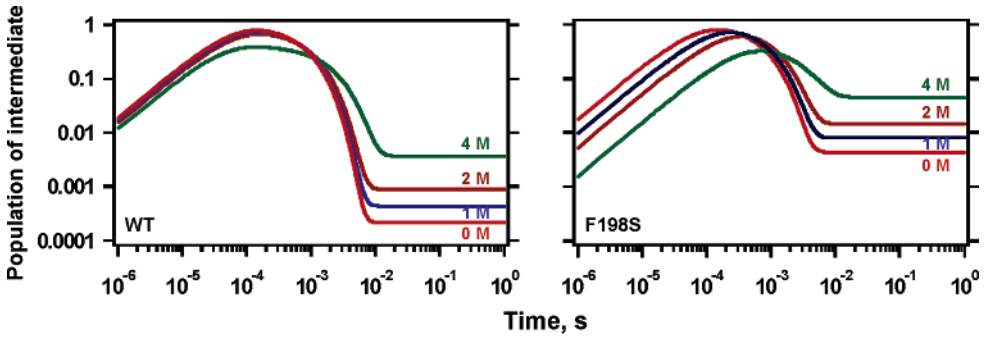

Figure 5. Time-dependent evolution of the population of the intermediate state, I, during refolding of wild-type huPrP90-231 (left panel) and the F198S variant (right panel) at different urea concentrations in 50 mM phosphate buffer, pH 7. Simulations were performed as described in the Materials and Methods section. Numbers by each curve indicate the concentration of urea.

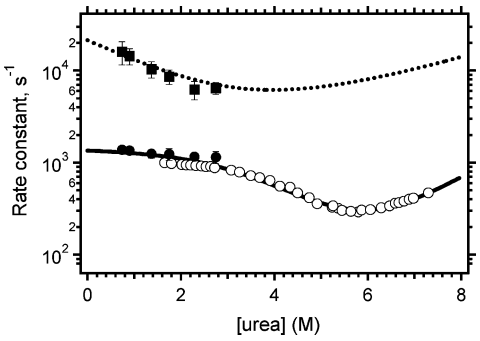

Figure 6. Urea concentration dependence of rate constants for folding/unfolding of huPrP90-231 at pH 4.8. (■) and (●) represent rate constants for fast and slow refolding phases, respectively, as observed in continuous-flow experiments; (○) represent rate constant for the single folding/unfolding phase observed in stopped-flow experiments. All rate constants were measured at 5 °C in 50 mM sodium acetate buffer, pH 4.8. Lines represent the best fit according to a three-state folding model (Scheme 1). The elementary rate constants and m values derived from the fit are: $k_{UI}^0 = 21{,}000$, $k_{IU}^0 = 680$, $k_{IN}^0 = 1390$, $k_{NI}^0 = 4.5$, $m_{UI}^{\neq} = 0.3$, $m_{IU}^{\neq} = 0.2$, $m_{IN}^{\neq} = 0.02$ and $m_{NI}^{\neq} = 0.35$. Rate constants and m values are given in s^{-1} and kJ mol^{-1} M^{-1}, respectively.

subject to considerable error. Therefore, we have re-examined the folding of huPrP90-231 at pH 4.8 using the continuous-flow method. As in the case of experiments at neutral pH, the kinetic traces at pH 4.8 were well represented by double-exponential functions. Furthermore, the denaturant dependence of the observed rate constants for the fast and slow phases could be well described according to a three-state folding model, yielding parameters described in the legend to Figure 6. Simulations of experimental data to calculate the population of folding intermediate as a function of time (similar to the one depicted in Figure 5A for huPrP90-231 folding at pH 7) indicate that, under conditions corresponding to an equilibrium in the absence of any denaturants, the intermediate at pH 4.8 accumulates at the level of approximately 1:300 molecules (as compared to ~1:10 000 at pH 7.0). The population of the intermediate becomes even higher in the presence of urea, increasing to 1:90 and 1:25 molecules in 2 and 4 M urea, respectively.

Discussion

A persistent controversy in prion research relates to the normal folding pathway of the prion protein and the nature of direct monomeric precursor that converts to the oligomeric, β-sheet-rich PrP^{Sc} state. The formation of amyloid fibrils in a number of other proteins is known to be mediated by monomeric, partially folded intermediate states whose population is usually enhanced by disease-related mutations.[38−40] In the case of the prion protein, however, detection and characterization of putative monomeric intermediates proved to be difficult. In fact, initial studies have concluded that PrP folds by a two-state mechanism without any intermediates, postulating that it is the fully unfolded state that is directly recruited into the PrP^{Sc} oligomer.[22,41] Only recently has experimental evidence started to emerge indicating the involvement of partially structured monomeric species in prion protein folding and misfolding.[23,24,42−44] A significant part of this evidence comes from kinetic stopped-flow experiments.[23,24] However, detailed interpretation of kinetic data has been hampered by the very fast rate of prion protein folding, with a major part of the reaction occurring within the dead time of conventional stopped-flow instrumentation. In an effort to overcome this difficulty and other uncertainties in interpretation of stopped-flow data, here we have employed an ultrafast continuous-flow mixing method which allowed us to extend kinetic measurements to early folding events. The present data provides direct and unambiguous evidence for accumulation of a partially structured intermediate in early stages of prion protein folding. Formation of this intermediate, at a rate of ~20 000 s^{-1}, is followed by a slower folding step occurring on the millisecond time scale.

The extremely fast rate of early events in prion protein folding is consistent with recent data indicating residual structure in PrP under denaturing conditions; this residual structure might act as a "template" for the native structure, thus accelerating the folding process.[44] However, although the present continuous-flow results are fully consistent with—and best described by—a sequential three-state model involving an on-pathway (obligatory) intermediate (Scheme 1), one cannot rule out alternative mechanisms involving formation of early nonproductive states (off-pathway intermediates) or mechanisms with parallel pathways. Rigorous discrimination between these alternative models

(38) Kelly, J. W. *Curr. Opin. Struct. Biol.* **1998**, *8*, 101−6.
(39) Booth, D. R.; Sunde, M.; Bellotti, V.; Robinson, C. V.; Hutchinson, W. L.; Fraser, P. E.; Hawkins, P. N.; Dobson, C. M.; Radford, S. E.; Blake, C. C.; Pepys, M. B. *Nature* **1997**, *385*, 787−93.
(40) Canet, D.; Last, A. M.; Tito, P.; Sunde, M.; Spencer, A.; Archer, D. B.; Redfield, C.; Robinson, C. V.; Dobson, C. M. *Nat. Struct. Biol.* **2002**, *9*, 308−15.
(41) Hosszu, L. L.; Baxter, N. J.; Jackson, G. S.; Power, A.; Clarke, A. R.; Waltho, J. P.; Craven, C. J.; Collinge, J. *Nat. Struct. Biol.* **1999**, *6*, 740−3.
(42) Nicholson, E. M.; Mo, H.; Prusiner, S. B.; Cohen, F. E.; Marqusee, S. *J. Mol. Biol.* **2002**, *316*, 807−15.
(43) Kuwata, K.; Li, H.; Yamada, H.; Legname, G.; Prusiner, S. B.; Akasaka, K.; James, T. L. *Biochemistry* **2002**, *41*, 12277−83.
(44) Hosszu, L. L.; Wells, M. A.; Jackson, G. S.; Jones, S.; Batchelor, M.; Clarke, A. R.; Craven, C. J.; Waltho, J. P.; Collinge, J. *Biochemistry* **2005**, *44*, 16649−57.

has been possible only in very few cases of model proteins (e.g., bacterial immunity protein Im7[45]), for which there is a tight coupling between the fast and slower folding events, and spectroscopic properties of the native, intermediate, and unfolded ensembles are very different (see ref 31 for further discussion). Unfortunately, these rare conditions are not met for the prion protein.

While the intrinsic limitations of kinetic experiments leave a degree of uncertainty as to whether an early folding intermediate represents a productive and obligatory species in *normal folding* of the cellular prion protein, the evidence for accumulation of this intermediate has important implication with respect to the mechanism of PrP^{C} conversion into the *misfolded* PrP^{Sc} aggregate. Partially structured folding intermediates are usually characterized by a large exposure of the polypeptide backbone to solvent and relatively high hydrophobicity, enabling intermolecular interactions. Thus, regardless of its specific role in the formation of the unique native structure of PrP^{C}, the partially folded intermediate is a "natural" candidate for a monomeric species that is directly recruited into the aggregated state and, eventually, converts to β-sheet-rich PrP^{Sc} structure. The role of this intermediate in the $PrP^{C}\rightarrow PrP^{Sc}$ conversion is further supported by the finding that the intermediate state for PrP variants associated with familial cases of Creutzfeldt−Jakob and Gerstmann−Straussler−Scheinker diseases has increased stability and is thus more highly populated. This effect, first inferred from our stopped-flow data,[24] has now been directly confirmed by a more rigorous approach involving continuous-flow measurements. The present experiments also demonstrate a profound stabilization of the intermediate relative to the native state at mildly acidic pH, correlating nicely with observations that the transition of the recombinant prion protein to β-sheet-rich oligomers[33,46] and amyloid fibrils (Patel, S., Apetri, A. C., Surewicz, W. K., unpublished data) is strongly promoted under acidic conditions. This is potentially of direct relevance to prion disease pathogenesis, especially in view of previous reports suggesting the involvement of acidic compartments in the $PrP^{C}\rightarrow PrP^{Sc}$ conversion reaction.[47]

Acknowledgment. This work was supported by NIH grants NS38604 and NS44158 (to W.K.S.) and GM056250 and CA06927 (to H.R.), and an appropriation from the Commonwealth of Pennsylvania to the Fox Chase Cancer Center.

JA063880B

(45) Capaldi, A. P.; Shastry, M. C.; Kleanthous, C.; Roder, H.; Radford, S. E. *Nat. Struct. Biol.* **2001**, *8*, 68−72.
(46) Swietnicki, W.; Morillas, M.; Chen, S. G.; Gambetti, P.; Surewicz, W. K. *Biochemistry* **2000**, *39*, 424−31.
(47) Caughey, B.; Raymond, G. J.; Ernst, D.; Race, R. E. *J. Virol.* **1991**, *65*, 6597−603.